REVIEW

National Science Open
1: 20220026, 2022
https://doi.org/10.1360/nso/20220026

Information Sciences

Special Topic: Novel Optoelectronic Devices

Advances of semiconductor mode-locked laser for optical frequency comb generation

Wenqi Wei[1,2], Jiajian Chen[2], Jingzhi Huang[1], Zihao Wang[1,2], Jianjun Zhang[1,2] & Ting Wang[1,2,*]

[1]*Institute of Physics, Chinese Academy of Sciences, Beijing 100190, China;*
[2]*Songshan Lake Materials Laboratory, Dongguan 523808, China*

*Corresponding author (email: wangting@iphy.ac.cn)

Received 19 May 2022; Revised 6 July 2022; Accepted 29 July 2022; Published online 23 September 2022

Abstract: Semiconductor mode-locked lasers (MLLs) can provide coherent optical frequency combs (OFCs) with high repetition rates and output power, which have been recognized as potential multi-wavelength sources used in optical communication field due to their compactness, high-efficiency, and low-cost properties. In this article, we have reviewed recent development of semiconductor MLL-based frequency comb generation. Different approaches of semiconductor MLLs for OFC generation are synoptically summarized based on various material platforms. The representative progress of III-V semiconductor MLLs on III-V platform and especially on Si substrates is both discussed for the applications in integrated silicon photonics.

Keywords: optical frequency combs, semiconductor mode-locked lasers, silicon-based photonic integrated circuits, monolithic and heterogeneous integration

Introduction

Over the past decade, following the emergence of mode-locked laser (MLL) [1] and high-Q micro-ring resonators, optical frequency combs (OFCs) have attracted significant research interest owing to their outstanding optical properties. As known, OFCs were initially developed for precision measurements, such as optical ruler and atomic clocks [2–4]. By providing the combs with finest precision, OFCs can be utilized to conduct fine precision measurement since they can transfer phase and frequency information from stable references to optical domain, ultrafast pulse generation, calibration of atomic spectrographs [5]. The last decades witness numerous applications of OFCs in various fields, such as medical diagnostics [6], precision measurements [7,8], gas spectroscopy [9,10], and optical communications [11–14]. Meanwhile, in order to meet the desire of application divergence, different laser-based comb technologies are developed [15], including gain switched comb [16,17], nonlinear fibers [18], high-Q microresonators [19,20], electro-optic comb generators [21,22], and semiconductor MLLs [23–27].

Nowadays, OFCs have been recognized as potential multi-wavelength sources used in optical communication field, which can provide up to thousands of optical channels from single comb laser applied in dense

wavelength-division multiplexing (DWDM) systems [20,28–30]. However, the traditional OFC-based technologies mainly rely on the bulky, power-hungry, complex, and expensive equipment to generate the comb lines, which will seriously restrict the application of them. Fortunately, with the rapid development of silicon-based photonic integrated circuits (PICs) [31], the OFC light sources can be produced by utilizing the advanced nanofabrication techniques based on the micro-ring resonators [20]. With these advantages mentioned above, OFC systems are becoming much more compact, power-efficient, and economic [32]. This leads OFC devices into the consumable applications, such as autonomous driving [33], biological recognition [34], and 5G/6G communications [35].

During the development in the last few decades, many achievements have been made to produce OFCs based on integrated photonics. Generally, there are two main categories in integrated photonics to generate comb sources: nonlinear frequency combs [36,37] and semiconductor MLLs [23,38]. For the nonlinear OFCs, various nonlinear optical media are adopted to generate the comb lines, such as Si [39], SiO_2 [40], Si_3N_4 [41], AlN [42], AlGaAs [43], $LiNbO_3$ [44], and SiC [45]. Benefiting from the mature photonic platforms, nonlinear OFCs exhibit essential advantages of scalability, compactness, and low cost. On the other hand, the passive photonic devices generated OFCs always require the external optical pump lasers, which will bring drawbacks in some emerging on-chip application fields that require monolithic integration and low power consumption [46]. By contrast, semiconductor MLLs are considered a promising comb source for future PICs due to their improved compactness, low power consumption, great fabrication tolerance, and cost efficiency [11,31,47].

In this article, we focus on the semiconductor MLLs for generation of OFC light sources. Different comb-generating techniques of semiconductor MLLs are compared here, while recent advances in integrated OFCs based on various material platforms are reviewed. The overall challenges and outlooks of integrated OFC sources in the near future are discussed.

Overview of semiconductor mode-locked lasers

Fundamental mechanisms of semiconductor MLLs

It is known that semiconductor MLLs are a special type of diode lasers, which provide coherent output comb lines with all the phase-locked longitudinal modes and equally-spaced frequency spectra [48]. All the optical modes in the OFC spectra can be described by the two basic metrics: repetition frequency and offset frequency. The repetition frequency defines the light emission frequency, and the offset frequency represents the additive frequency to achieve a harmonic and coherent operation among all optical modes. This offset comprises the difference in group velocity of different longitudinal modes so that they share a common phase and thus form laser pulses. Simply speaking, the repetition frequency represents the periodicity of the OFC line train. The offset frequency describes the phases of every individual mode, and allows fine optical frequency control. For most applications, the repetition rate should be suitable with the electronics used in signal detection and processing, which usually owns the order of tens of gigahertz or less in RF frequencies.

So far, remarkable achievements have been made in the development of semiconductor MLLs. In the following text, the four mode-locking mechanisms about semiconductor MLLs are briefly introduced.

Active mode locking

For active MLLs, an RF electrical modulation signal is applied by inserting the as-grown modulation gain section or an optical modulator in the laser cavity [49,50], as shown in Figure 1A. As the frequency of the electrical modulation signal is close to the laser cavity roundtrip frequency, the gain of the laser is larger than the loss introduced by the modulator and the optical pulses can be achieved from the device. During operation, the complex longitudinal modes in the laser cavity will be modulated by the RF input and an equidistant modulation sideband mode will be acquired. At last, all the lasing modes will couple together by the frequency pulling effect [51] and stable mode-locked state will be presented. Active mode locking is favored in electro-optic applications, because both the modulation strength and frequency can be controlled by the electrical modulation signal to enable both frequency and phase modulation formats.

Passive mode locking

To obtain the passive mode locking mode, a saturable absorber (SA) is always introduced in the laser cavity as a nonlinear absorption component [52] as shown in Figure 1B. The SA consists of a part of the active region, which is controlled by a reverse bias and electrically isolated from the laser gain section. As the conduction and valence of the laser SA section are fully filled with carriers coming from an optical pulse with high intensity, the SA part will be bleached and suppress further absorption of photons. Meanwhile, because of the absorption loss, the continuous-wave (CW) optical source does not experience net gain, and the

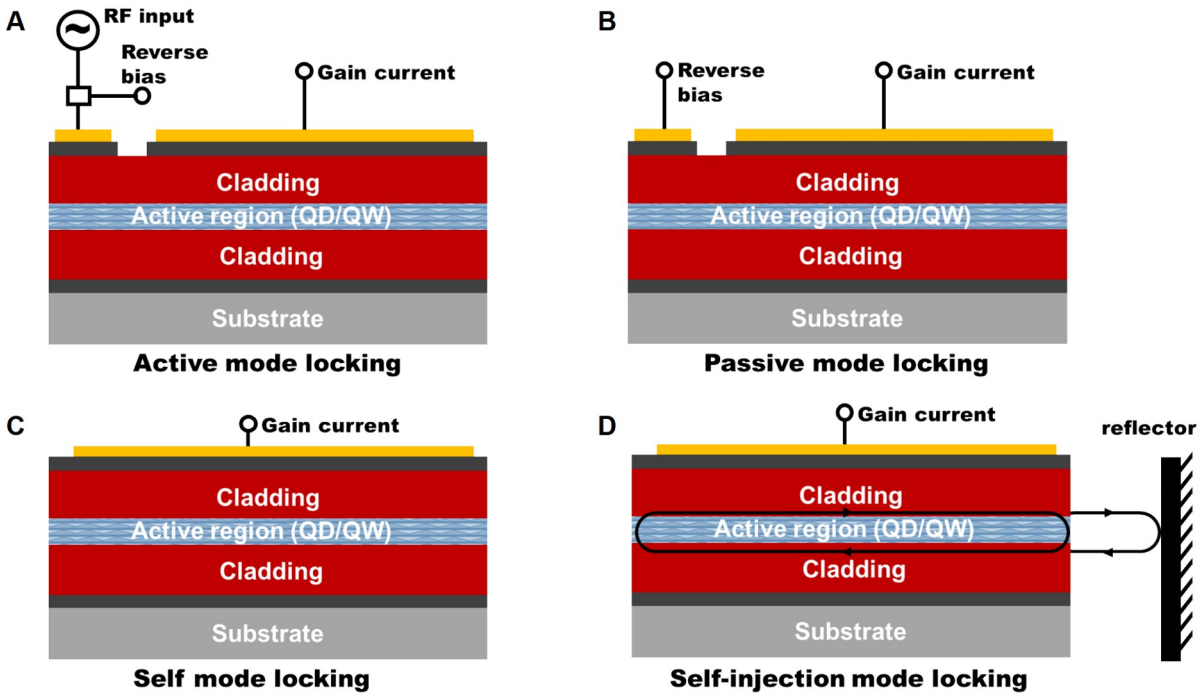

Figure 1 Four mode-locking mechanisms for semiconductor MLLs [50]. (A) The schematic configurations of the four mode-locking mechanisms: (A) active mode locking, (B) passive mode locking, (C) self-mode locking mode, and (D) self-injection mode locking.

transient noise spike can bleach the absorption loss in the laser cavity to form a net gain window, ultimately leading to the building-up of pulse oscillation [48]. Moreover, the SA can also function as an attenuator which will shorten the duration of the pluses by absorbing the leading wing of the circulating pulse and balance other pulse broadening effects such as chromatic dispersion, resulting in an ultra-short pulse line. Owing to its desirable properties described above, passive mode locking has been the most widely used mode-locking strategy recently.

For the passive mode locking, the SA section was set at the tail end of the laser, and the repetition rate is the same as the free spectral range (FSR) of the laser cavity. In actual applications requiring a higher repetition rate, the gain section cavity length must be shortened to increase the FSR, which is undesired because the optical gain of a shorter gain section may not be large enough to overcome the overall loss of the device. To address this issue, the colliding-pulse mode locking (CPML) strategy was introduced by inserting multiple SA sections at specific integer fractions of the cavity length to realize a harmonic mode-locking operation, which enables up to hundreds of GHz repetition rates in cavities with a much lower fundamental frequency [53].

Self-mode locking

Different from active and passive mode locking methods, self-mode locking can be directly obtained only by a single-section laser structure without any modulation signals as shown in Figure 1C. Avoiding use of SA sections which will increase the intracavity loss of the laser, the OFCs generated by self-mode locking own higher power and efficiency. The most common self-mode locking behavior can be realized by strong four-wave mixing (FWM) within the active materials combined with the spatial hole-burning effect [54,55] in a Fabry-Perot (FP) cavity. Due to this effect, one important application of self-mode locking is for mode-locked quantum cascaded lasers (QCLs) at longer lasing wavelength (>3 μm) where the ultrashort excited-state lifetime prevents passive mode locking. Moreover, the self MLLs always exhibit superior coherence over other comb lines, and they do not necessarily produce single pulses with a uniform phase throughout the frequency spectrum.

Self-injection mode locking

Self-injection locking is a dynamic phenomenon representing stabilization of the emission frequency of a laser diode with a passive cavity enabling itself frequency-filtered coherent feedback to the laser cavity. Figure 1D shows the schematic configuration of the self-injection MLLs with an external feedback reflector, such as optical fiber loop and high-Q resonators. Meanwhile, the linewidth of the laser could be decreased down to Hz range [56]. In this review, the Si-based InAs/GaAs quantum dot (QD) self-injection MLLs will be demonstrated to generate OFCs with narrow line width and tunable spacing rates.

Material platforms for semiconductor MLLs

Quantum well semiconductor MLLs

The first integrated semiconductor MLL was demonstrated based on quantum well (QW) structures oper-

ating at 1.5 μm wavelength [38]. Over the past decades, with the significant development of semiconductor lasers, there have been many demonstrations of QW-based semiconductor MLLs with the lasing wavelengths covering the visible to near-infrared bands. Here, some research results of QW-based semiconductor MLLs will be reviewed according to the material categories.

InGaN/GaN [57]**.** By using a triple-section self-pulsating InGaN/GaN QW-based laser diode (SP-LD) operated by dc bias, the optical pulses were shortened to 15 ps with the emission wavelength of 402 nm and the optical peak power became as high as 10 W with a pulse repetition frequency of 1 GHz. This work provides a simple scheme to generate a picosecond optical pulse at a gigahertz repetition frequency without an external optical modulator component.

AlGaAs/GaAs [58]**.** The monolithic multi-sectioned AlGaAs/GaAs QW laser operating as multiple colliding pulse mode-locking source with lasing wavelength at around 868 nm was reported in ref. [56]. High-repetition-rate pulse trains (up to 375 GHz) were achieved with the pulse width of about 1 ps. Moreover, the spectrum consisting of three modes gives a time-bandwidth product of <0.5.

AlGaInAs/InP [59]**.** By inserting a transparent passive waveguide in part of the AlGaInAs/InP QW laser cavity, the OFCs with 490-fs pulse width and 1550 nm-band light emission were achieved, which is the shortest pulse width reported based on QW MLLs. Moreover, several approaches are described for the harmonic mode-locking (HML) strategy: colliding pulse ML operating up to 240 GHz, coupled cavity ML up to 160 GHz, and sampled Bragg grating constructions up to 1.28 THz. These approaches offer a stable HML operating from 40 GHz to >1 THz. Finally, the synchronized multi-wavelength ML laser array was demonstrated, which contains four 40-GHz lasers with designed wavelength registration used for optical code division multiple access or optical time division multiple access applications.

Quantum dot semiconductor MLLs

Although QW-based semiconductor MLLs have been intensively investigated over the last two decades, the advent of QD material systems has attracted much research attention. Benefiting from the three-dimensional confinement of carriers, QDs exhibit a delta-function-like density of states, which enable unique physical properties of ultra-fast carrier dynamics, lower threshold current density, reduced sensitivity to crystalline defects, improved stability against optical feedback, and low temperature sensitivity [60–67]. Additionally, the semiconductor lasers with QD gain materials own the low relative intensity noise (RIN), leading to a large signal-to-noise ratio (SNR) and a low bit-error rate of the optical lines, which is required in the high-speed communication systems [68]. Furthermore, the inhomogeneous nature of the self-assembled QDs will broaden the gain spectrum, which is advantageous for broadband comb generation. Among all the attributes, one of the most notable properties is that the insensitivity to defects allows direct-epitaxial integration of high-quality QD MLLs on silicon substrates for PICs [69].

Typical QD-based structures (InAs/GaAs and InAs/InGaAsP) can cover the wavelength range from 1.1 to 1.8 μm, while for application at longer wavelengths (>3 μm), interband cascade lasers or QCLs should be conducted. In terms of QCL-based OFCs, it is challenging to achieve the standard two-section passive MLLs, due to the fast gain recovery (~0.3 ps) [70], which is much shorter than the cavity roundtrip time. The active or self-mode locking strategies can be applied to obtain combs from QCLs [71].

In the past decade, impressive achievements have been made in the field of InAs/GaAs or InAs/InGaAsP

QD-based MLLs with high repetition rate ranging from tens to hundreds of gigahertz. Despite phenomenal success of semiconductor MLLs at the device level, incorporating the OFC sources into the PICs is still challenging. There are two major approaches to integrating OFCs with other passive photonic components in PICs: monolithic or heterogeneous integration. Owing to the QD insensitivity to defects described above, epitaxial growth of QD-based light sources with telecom O and C band on complementary metal-oxide semiconductor (CMOS)-compatible Si (001) and SOI substrates is becoming possible, namely monolithic integration, which is considered one of the promising routes for future PICs. In comparison, heterogeneous integration of multiple photonic devices has great advantages of flexibility and relatively mature fabrication process, but can be challenging in large-scale foundry production [72].

Table 1 summarizes some representative research results regarding III-V semiconductor comb sources [73–83]. Both the O-band and C-band III-V semiconductor mode-locked OFCs with high repetition rates and narrow linewidth are demonstrated.

III-V MLLs on GaAs and Si for integrated comb source

Passive MLL comb source on GaAs (001) substrate

The passive mode locking is one of the traditional methods to provide on-chip comb source due to its simplicity, handleability and compactness. The typical FP-cavity lasers can act as comb sources by introducing a SA, which conducts as a nonlinear absorption component in the cavity [52]. In practice, the SA can be realized by reverse biasing one part of the active region of the FP laser, which should be electrically isolated from adjacent gain sections. Taking advantages of these specially designed passive mode-locking III-V semiconductor MLLs with single or multi SAs, great achievements have been made with tens to several hundreds of gigahertz repetition rates, which cover the O and C band telecommunication wavelengths [71,74,76,84].

Due to the delta-function-like density of states of QDs [85], the QD-based III-V lasers own high temperature stability, and high-temperature up to 220°C CW operation has been reported for an InAs/GaAs QD FP laser [63]. Nowadays, with the rising demands of DWDM systems, the comb spacing of MLLs must be stable enough over an extremely broad temperature range. Stable mode-locking from 20°C to 92°C has been reported from a two-section InAs/GaAs QD passive MLL on GaAs [86], but with a 20.5 GHz repetition rate, which is not large enough to meet the minimum requirement (e.g., 25 GHz) of DWDM application. In 2020, the group from University College London demonstrated an ultra-stable frequency comb source based on a two-section InAs QD passive MLL with 25.5 GHz repetition rate over a broad temperature range of 20°C–120°C [77]. Figures 2A and 2B show the schematic and SEM image of the passive two-section InAs/GaAs QD MLL device. The InAs QD laser structure was optimized to achieve high optical gain and large energy separation between GS (ground state) and ES (excited state), which will provide considerable output power and suppress the mode-locking switching between the two states at an elevated temperature range. A 1615 μm long laser cavity with a 200 μm long SA was conducted to obtain a fundamental repetition rate of 25 GHz. The RF spectra (Figure 2C) show a 0.07 GHz change in mode spacing over the extremely broad temperature range from 20°C to 120°C, which is the broadest temperature range ever reported. A stable coherent comb spectrum with a lasing wavelength of 1349 nm and a −6 dB comb bandwidth of 4.81 nm was

Table 1 Summary of III-V semiconductor mode-locked OFC sources with high comb spacing

Operation principle	Configuration	Optical linewdith	Comb spacing	Bandwidth	Ref.
Passive Mode-locking	InGaAsP MQW with extended Si cavity	400 kHz	100 Mhz–1 GHz	12 nm (10 dB)	[73]
Passive Mode-locking	InP/InAlGaAs MQW with extended SiN cavity	200 kHz	755 MHz	3.27 nm (10 dB)	[74]
Passive Mode-locking	InAs/GaAs QD on SOI with external cavity	N/A	102 GHz	6.5 nm (3 dB)	[75]
Passive Mode-locking	5th-order InAs chirped QD CPML on Si	N/A	100 GHz	N/A	[76]
Passive Mode-locking	Two-section InAs QD MLL	N/A	25.5 GHz	4.7 nm (6 dB)	[77]
Passive Mode-locking	Two-section InAs QD MLL	N/A	94 GHz	3.18 nm (3 dB)	[78]
Passive Mode-locking	4th-order InAs/GaAs QD CPML	440 kHz	100 GHz	11.5 nm (3 dB)	[79]
Mono-wavelength Self-injection Locking	III-V DFB laser/SiN ring resonator	1.2 Hz	30 GHz	4 nm (10 dB)	[80]
Mono-wavelength Self-injection Locking	III-V MQW FP laser/SiN ring resonator	370 Hz	12.5 GHz	N/A	[81]
Mono-wavelength Self-injection Locking	III-V MQW FP laser/SiN ring resonator	186 kHz	1.2 THz	N/A	[82]
Multi-wavelength Self-injection Locking	InAs QD FP laser on Si/external Lyot filter	20 kHz	30–700 GHz (Tunable)	13 nm (10 dB)	[83]

achieved at a high temperature of 100°C (Figure 2D), which enables a maximum of 31 potential channels with an OSNR of more than 36 dB. In order to achieve a larger mode-spacing (≥100 GHz), which is more desirable in the DWDM transmission systems, a short laser cavity is needed. The 100 GHz QD mode-locked OFC sources with 128 Gbit/s/λ PAM-4 transmission ability were also presented by using a similar passive two-section InAs QD MLL but with a short laser cavity of 405 μm [78,84].

However, limited by the small gain region of the MLL with short cavity, these comb sources cannot provide sufficient single channel output power, which is a key factor of the OFC systems. In typical optical links, high output power at each wavelength can enable a better system-level performance with higher SRN and lower bit error rate [29,50]. Meanwhile, the optical amplifiers can also be integrated after the comb sources to boost up the optical power [87,88]. To fundamentally solve this issue, the passive MLL with high-order CPML has been introduced recently [79]. As shown in Figure 3A, a 4th-order MLL design with 1580 μm cavity length and three SAs is implemented here to allow four colliding pulses traveling intracavity to produce 4th-order harmonic pulses at 100 GHz repetition rate. Top-flat spectra from the CPML laser can be achieved over a large temperature range from 20°C to 100°C (Figure 3B). Under the optimum operating condition, as large as 20 comb channels at 100 GHz spacing with 3 dB optical bandwidth of 11.5 nm are obtained as shown in Figure 3C, which have a record average optical linewidth of 440 kHz from the CPML. The high-speed external modulation of a single channel (1321.28 nm) from the 4th-order CPML was conducted as shown in Figure 3D, indicating open eye diagrams for 70 Gbits/s NRZ and 80 Gbits/s PAM-4 modulation formats with extinction ratios of 4.4 dB and 6.4 dB, respectively. The 4.8 Tbit/s data transmission is expected from the single 100 GHz CPML with 36 nm broadband spectrum containing maximum 60 channels over a variation of operation temperature. The CPML laser diode can provide stable OFC lines with large comb spacing, large 3 dB bandwidth and high output power, which would be widely used in WDM systems, optical interconnects, and photonic neural networks.

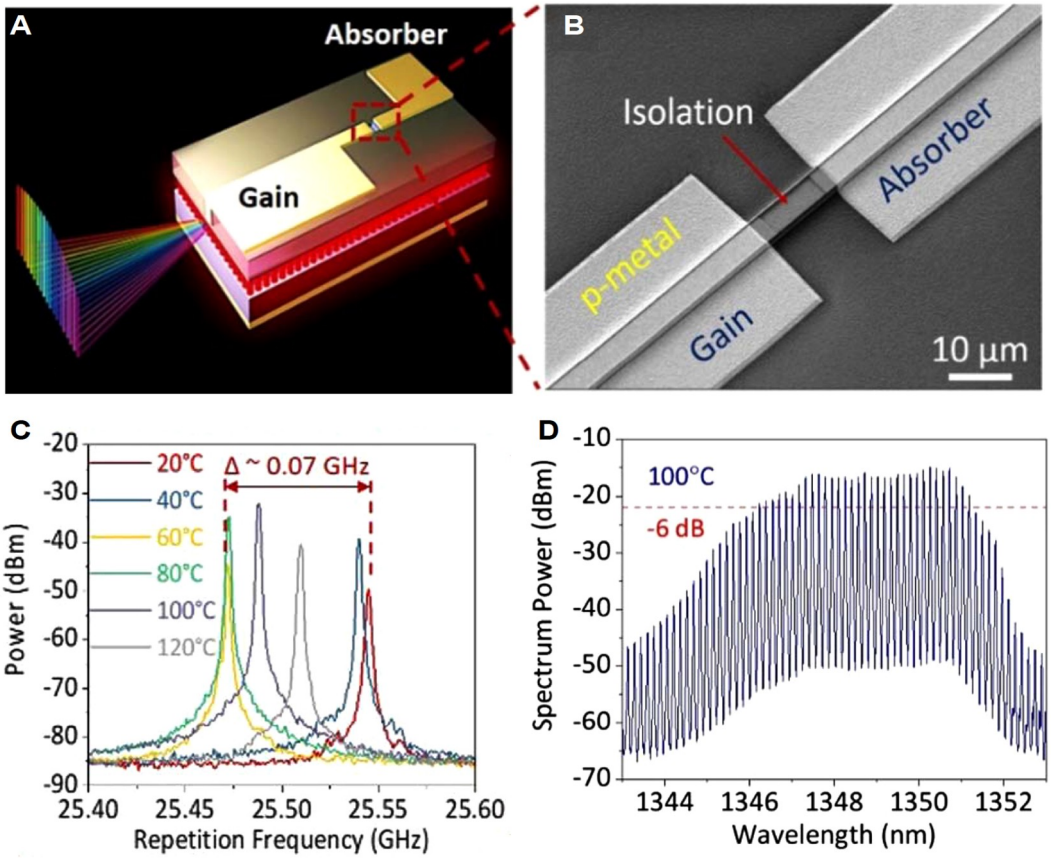

Figure 2 Ultra-stable 25.5 GHz InAs/GaAs QD MLL on GaAs (001). (A) and (B) Schematic of the passive two-section MLL, and SEM image of the device showing the gap between the gain and SA. (C) Temperature-dependent RF spectra. (D) Optical comb of the device at 100°C.

MLL comb sources on Si platforms

Compared with traditional fiber-based MLLs, the integrated MLLs on Si platforms provide the advantages of small footprint, low cost and operation simplicity for the DWDM systems used in silicon photonic integration. As mentioned above, both heterogeneous integration and monolithic integration play important roles in future highly dense PIC depending on applications.

Heterogeneous integration MLLs on Si

Heterogeneous integrated MLLs on Si platforms have been extensively explored in the last decade. In 2007, the two-section passive MLL bonded to a Si substrate was demonstrated by Koch *et al*. [25], which provides a C-band comb source with 40 GHz repetition rate and 4 ps pulses. The external cavity MLL was also employed to produce the comb lines with sharp linewidth and low phase noise. In 2017, Wang *et al*. [73] demonstrated a heterogenous ultra-dense MLL via III-V QW gain section bonded on silicon by utilizing DVS-BCB bonding method as shown in Figure 4. As shown in Figures 4A and 4B, the MLL consists of a long Si spiral waveguide (37.4 mm) with low loss (0.7 dB/cm), two optical amplifiers separated by a SA, and

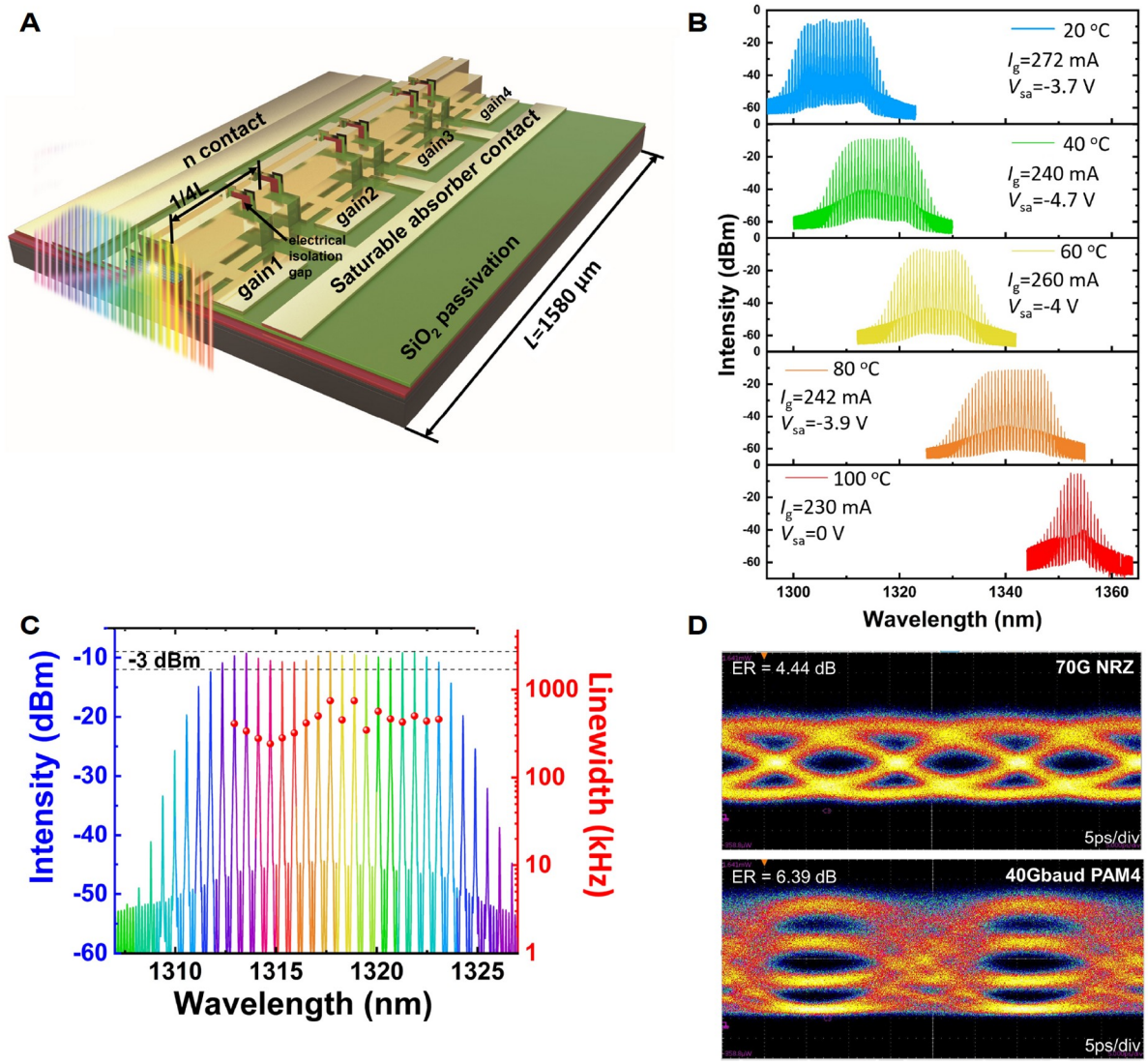

Figure 3 Fourth-order 100 GHz colliding pulse mode-locked InAs/GaAs QD laser (CPML) on GaAs (001). (A) Schematic of the passive 4th-order MLL. (B) Optical spectra evolutions with the temperature increasing from 20°C to 100°C. (C) Optical spectrum of flat-top QD-CPML under optimized bias condition. (D) 70 G NRZ and 40 Gbaud PAM-4 optical eye diagram using comb line at 1321.28 nm.

two distributed Bragg reflectors (DBR) acting as the mirrors of the cavity. Figure 4C shows the output spectrum when the laser is passively locked at 1 GHz repetition rate, indicating a 15 nm width 10-dB optical bandwidth and more than 1400 phase-locked comb lines. Recently, based on ultra-low loss Si_3N_4 external cavity, the III-V QW MLL on SOI with ultra-narrow RF linewidth was also reported by using the micro-transfer printing technique [74]. Cuyvers *et al*. [74] demonstrated a heterogeneous integrated III-V-on-SiN passively mode-locked laser with a narrow 755 MHz comb spacing, RF linewidth of 1 Hz and optical linewidth below 200 kHz. As shown in Figure 5A, the ultra-low losses of Si_3N_4 waveguides acting as external cavity were employed and the InP/InAlGaAs multi-QW active devices were transferred to the Si_3N_4 passive cavity chip. Figure 5B shows the RF spectrum of the passive MLL, presenting a top-flat densely-spaced RF comb spectrum with a 755 MHz line-spacing and exceeding 40 dB SNR. The zoom-in RF line with a center

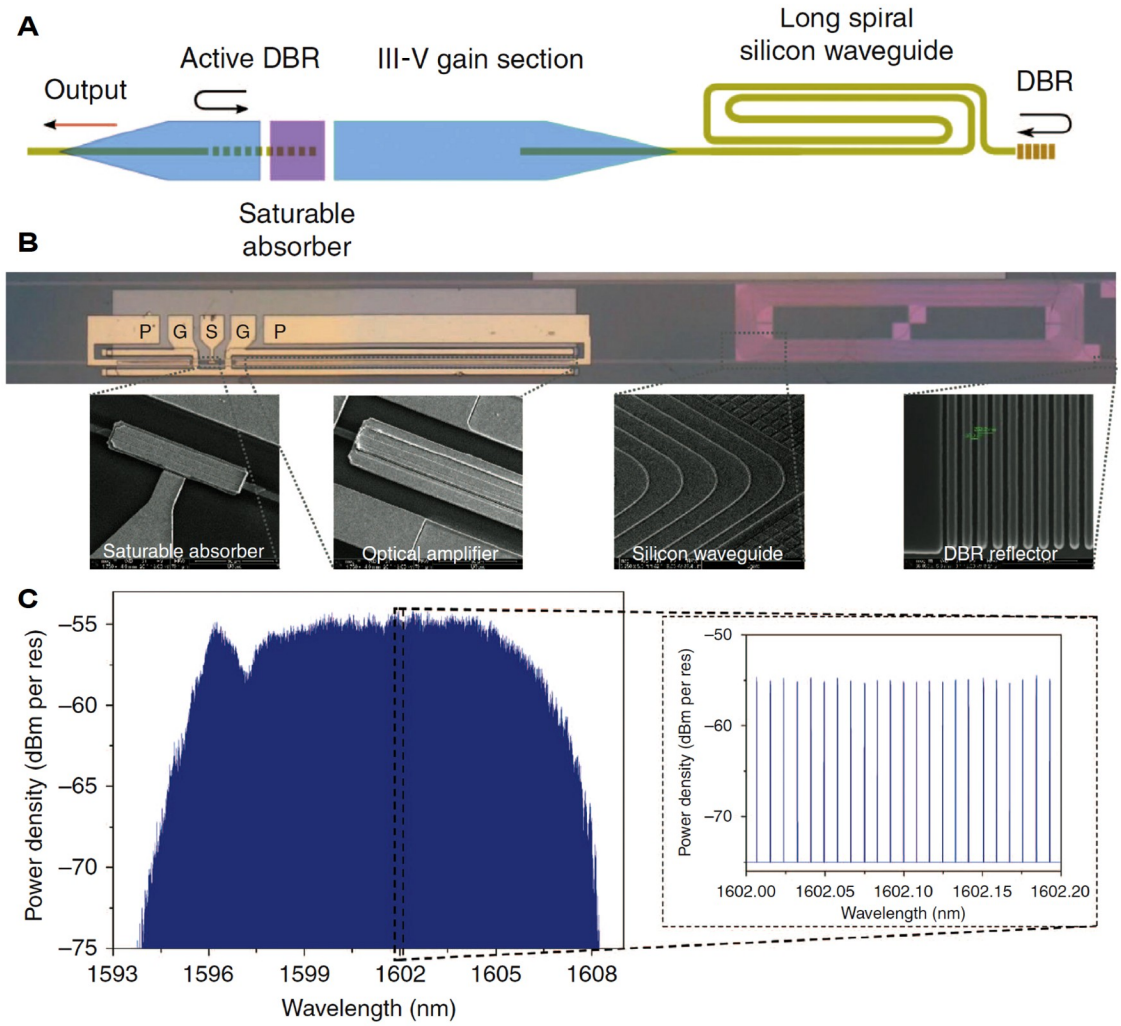

Figure 4 Heterogeneously integrated III-V-on-silicon passive MLLs. (A) Layout and (B) images of III-V comb laser heterogeneously integrated on SOI. (C) Output spectrum when the laser is passively locked at 1 GHz repetition rate.

frequency of 755.2 MHz is shown in Figure 5C, which displays a qualitative −10 dB RF linewidth of 300 Hz. The narrow RF linewidth indicates that all optical modes are tightly phase-locked. Additionally, the III-V QD-based MLLs were also realized on SOI substrates by Hewlett-Packard Laboratories via bonding technique [89–91]. The hybrid-silicon III-V quantum dot colliding pulse mode-locked lasers showed an error-free operation in multiple modes with extinction ratios of 11.5 dB, which can act as useful light sources with high-reliability in WDM optical links [90,91]. These results presented here proved a successful integration of ultra-low loss passive waveguides and III-V MLLs on SOI platform with massive comb channels and ultra-low phase noise.

Monolithic integration MLLs on Si

Although heterogeneously integrated III-V lasers on Si have been extensively demonstrated in recent years,

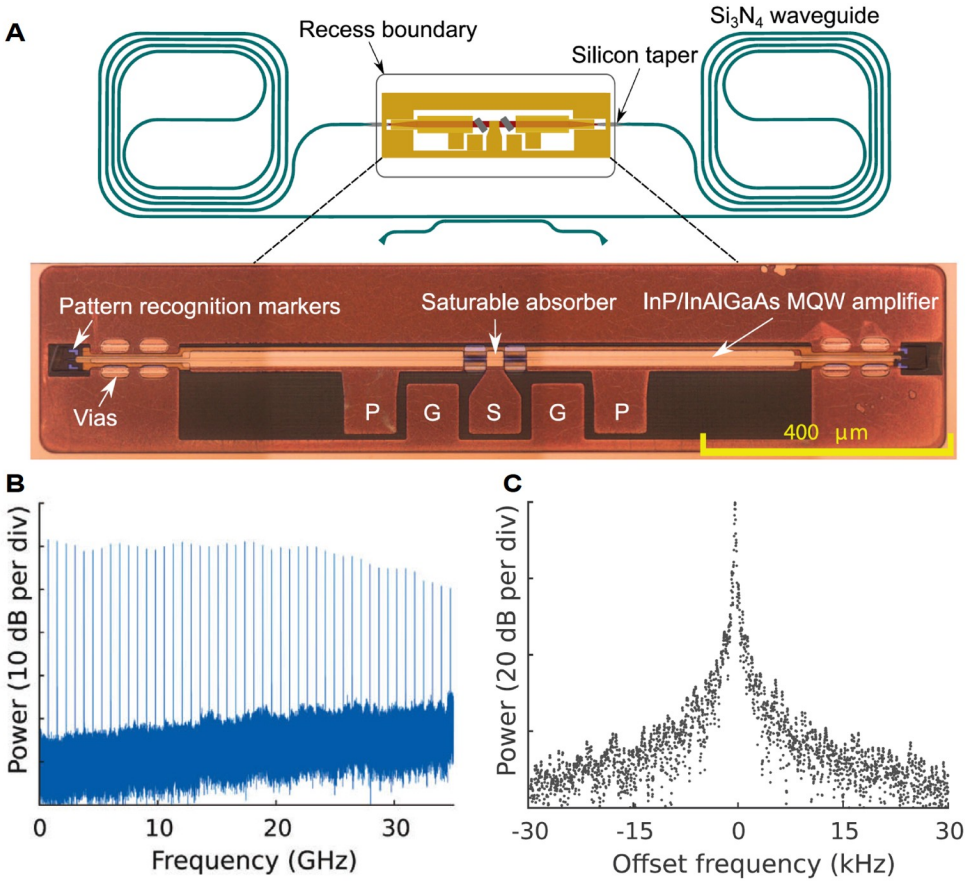

Figure 5 Heterogeneously integrated III-V-on-silicon-nitride passive MLLs. (A) Schematic of the device (upper) and microscope image of the III-V waveguide (lower); (B) RF spectrum of the generated pulse train; (C) zoom-in of the repetition frequency signal with a center frequency of 755.2 MHz.

monolithic integration has been considered an alternative solution to integrate III-V light sources, including MLLs on Si with high density and compactness. Due to the physical mismatch between III-V and Si, it is challenging to realize high-quality III-V materials epitaxially grown on Si substrates.

(1) III-V layers epitaxy on Si (001) substrates

In terms of epitaxial growth of III-V on Si, three major issues must be solved: threading dislocations (TDs), antiphase boundaries (APBs), and thermal cracks [92,93]. In the last 20 years, many techniques have been utilized for achieving high-quality III-V materials on IV substrates, and prominent achievements have been made towards high-performance InAs/GaAs QDs lasers grown on Si substrates with telecommunication wavelengths [94–98]. The off-cut silicon substrates (Figure 6A) were first used to avoid the formation of APBs when III-V was grown on Si, by producing double-atomic step surface under routine annealing process [94,95]. High-performance 1300 nm InAs/GaAs QD laser with a low threshold current density of 62.5 A cm^{-2} was then grown and fabricated on these substrates [99]. The patterned Si(001) substrates with high Miller index surfaces are also applied to avoid the APBs as shown in Figure 6B [100]. In addition, optimized AlGaAs nucleation layer [97] and special substrate surface treatments [101] are also adopted to avoid the APB formation as shown in Figures 6C and 6D. However, most techniques focused on the TD and

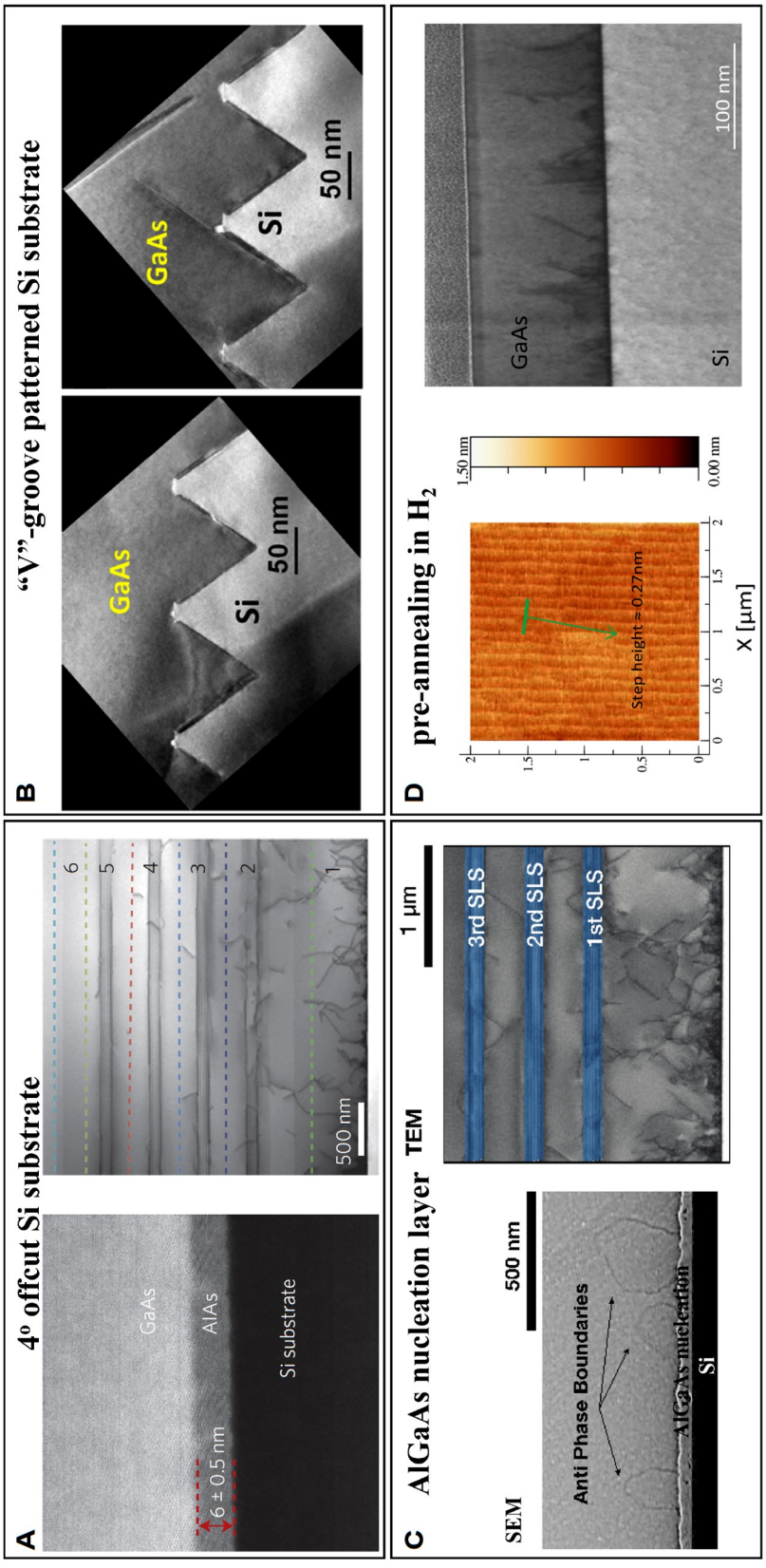

Figure 6 Techniques for epitaxial growth of III-V on Si platforms. (A) GaAs on an off-cut (2°, 4° or 6°) Si (001) substrates by MBE [90]. (B) GaAs on "V"-groove patterned Si (001) substrates by MOCVD [91]. (C) GaAs on Si (001) substrates with an AlGaAs nucleation layer by MBE [88]. (D) GaAs on the Si (001) substrates with double-atomic steps, produced by annealing the substrate in H_2 atmosphere in MOCVD [92].

APB suppressions, and the thermal crack issue remains unsolved.

In 2018, Wei *et al*. [102] demonstrated a novel epitaxial method by molecular beam epitaxy (MBE) to construct the (111)-faceted silicon hollow structures on the "U"-shaped patterned Si (001) substrates, and high-quality GaAs layers were achieved on Si (001) (Figure 7). As the cross-sectional TEM image shown in Figure 7D, the homoepitaxially-formed sawtooth structures can be effective to suppress APBs and reduce the TDs. From the AFM and ECCI measurement results shown in Figures 7E and 7F, no APBs were observed on the surface and a smooth GaAs layer with a 1.3 nm roughness (root-mean-square, RMS) and a 4.8×10^{6} cm^{-2} threading dislocation density was obtained after deposition of 2 μm III-V buffer on these specially designed Si (001) substrates. Moreover, the high-quality GaAs/SOI templates were also demonstrated by using the same method, and InAs/GaAs QD lasers were first grown and fabricated on SOI [103–105]. More importantly, the voids under the sawtooth structures shown in Figure 7C are experimentally proved to be able to release the thermal stress of the whole sample, avoiding the thermal crack formation. These high-quality GaAs/Si (001) platforms enable the possibility of growing and fabricating high-performance integrated InAs/GaAs QD light sources on CMOS-compatible Si (001) and SOI substrates for the applications in PICs.

(2) InAs/GaAs QD MLLs grown on Si (001) substrates

Owing to the dramatic progress in direct epitaxial growth of III-V on Si, the first passively mode-locked QD laser grown on Si substrates was demonstrated by Liu *et al*. [69] in 2019. Figure 8A shows the schematic diagram of the epitaxial structure on Si (001) substrate, including a 5-layer chirped QD active region in order to broaden the spectral bandwidth of the MLL. The 20 GHz two-section passive mode-locking design was conducted by using a 2048 μm cavity length with a 287 μm SA section as shown in Figure 8B. Figure 8C shows the square-like optical spectrum with the largest 3 dB bandwidth of 6.1 nm (58 lines, 80 lines within

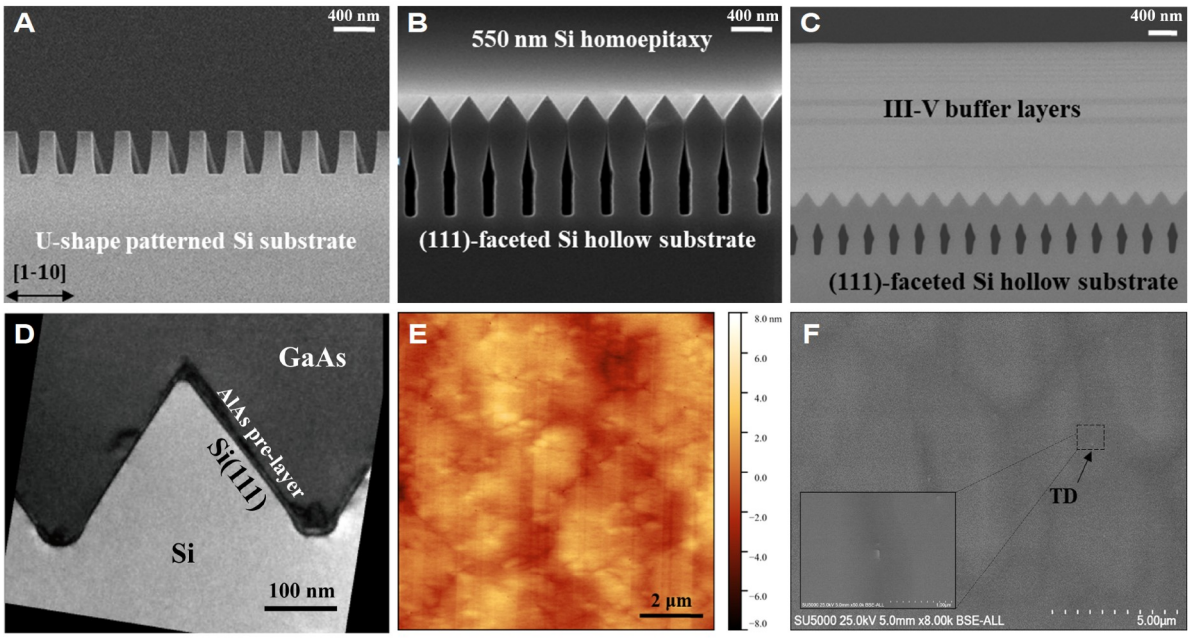

Figure 7 High-quality GaAs layers grown on Si (001) substrates. (A), (B), and (C) Cross-sectional SEM images of the "U"-shaped patterned Si (001), (111)-faceted silicon hollow substrate, and the GaAs/Si (001) substrate, respectively. (D), (E), and (F) Cross-sectional TEM image of the GaAs/Si interface, surface AFM and ECCI images of the GaAs/Si (001) sample, indicating a 1.3 nm RMS (root-mean-square) and a 4.8×10^{6} cm^{-2} threading dislocation density.

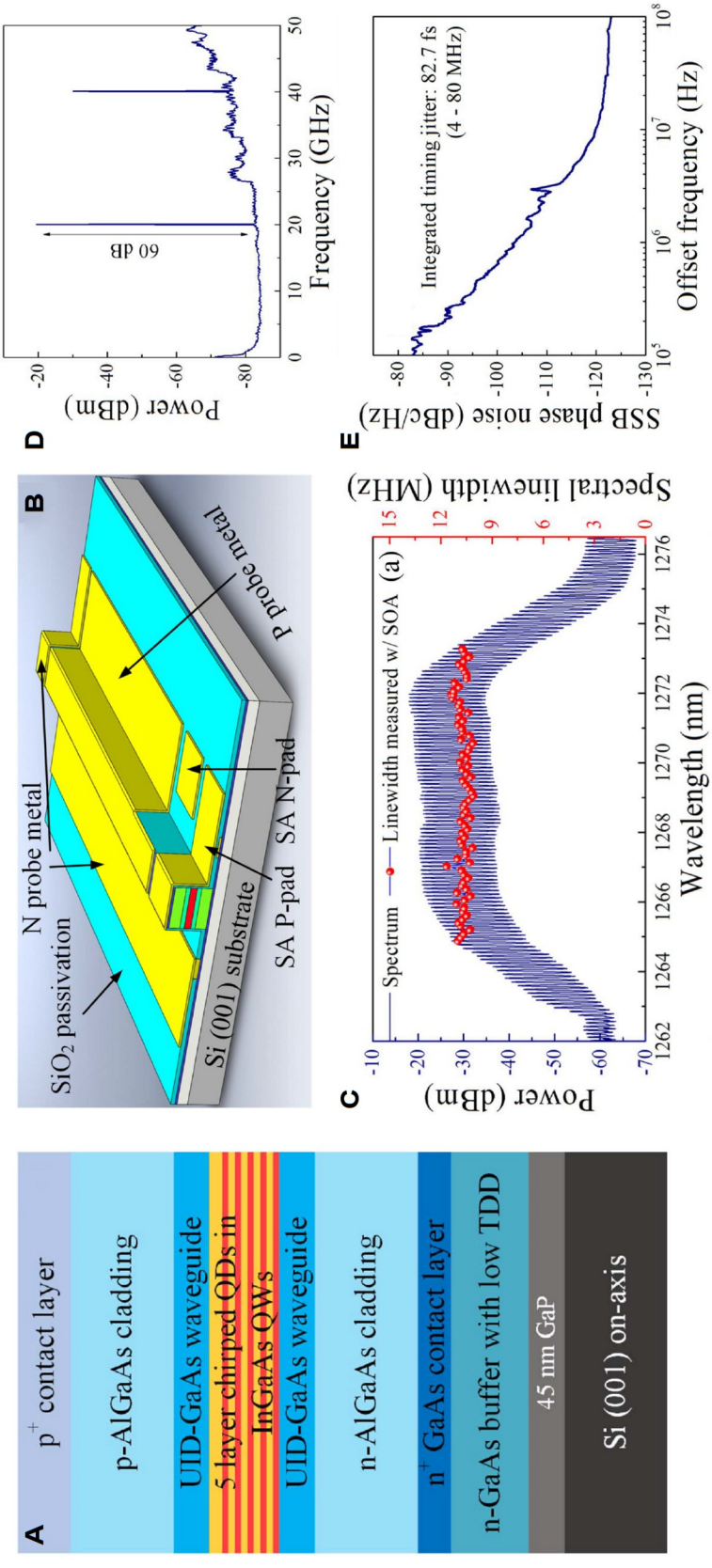

Figure 8 Si-based passively mode-locked 20 GHz QD-MLL. (A) and (B) Schematic diagrams of the epitaxial structure and the 20 GHz MLL device of quantum dot mode-locked laser on silicon, respectively. (C) Optical spectrum and corresponding optical linewidth of each mode within 10 dB. (D) RF spectrum in a 50 GHz span view. (E) The single-sideband phase noise plot under the narrowest pulse width condition.

10 dB) under optimized mode locking state of the Si-based MLL. A record low timing jitter value for the Si-based MLL of 82.7 fs (4–80 MHz) and a narrow RF 3 dB linewidth of 1.8 kHz are achieved as shown in Figures 8D and 8E. Although limited by the low repetition rate of 20 GHz, this work paves the way to integrate the on-chip MLL comb sources.

As known, in order to achieve high repetition rate MLL comb sources to avoid channel crosstalk, short laser cavity is needed, which suffers from reduced optical gain, especially for the lasers grown on Si substrates. It is difficult to obtain high-performance two-section InAs/GaAs QD passive MLL with high repetition rate (≥100 GHz) directly grown on Si substrate. In addition, MLL itself as an active comb source regularly experiences current and thermal induced frequency variation. Therefore, the self-mode locked QD lasers with assistance of self-mode locking technique can provide OFCs with narrowed optical linewidth, improved frequency and phase stability. Figure 9 shows a self-injection MLL, based on a standard InAs/GaAs QD FP laser grown on Si (001) substrate (Figure 9A) [27]. By introducing an optimized self-injection strength and proper phase, the RF linewidth of the MLL was significantly narrowed by two orders of magnitude from 900 to 8 kHz as shown in Figure 9C. For on-chip applications, this single-section Si-based InAs QD-MLL via optical self-injection can be realized by integrating a silicon photonic feedback loop with the laser diode to achieve coherent feedback conditions.

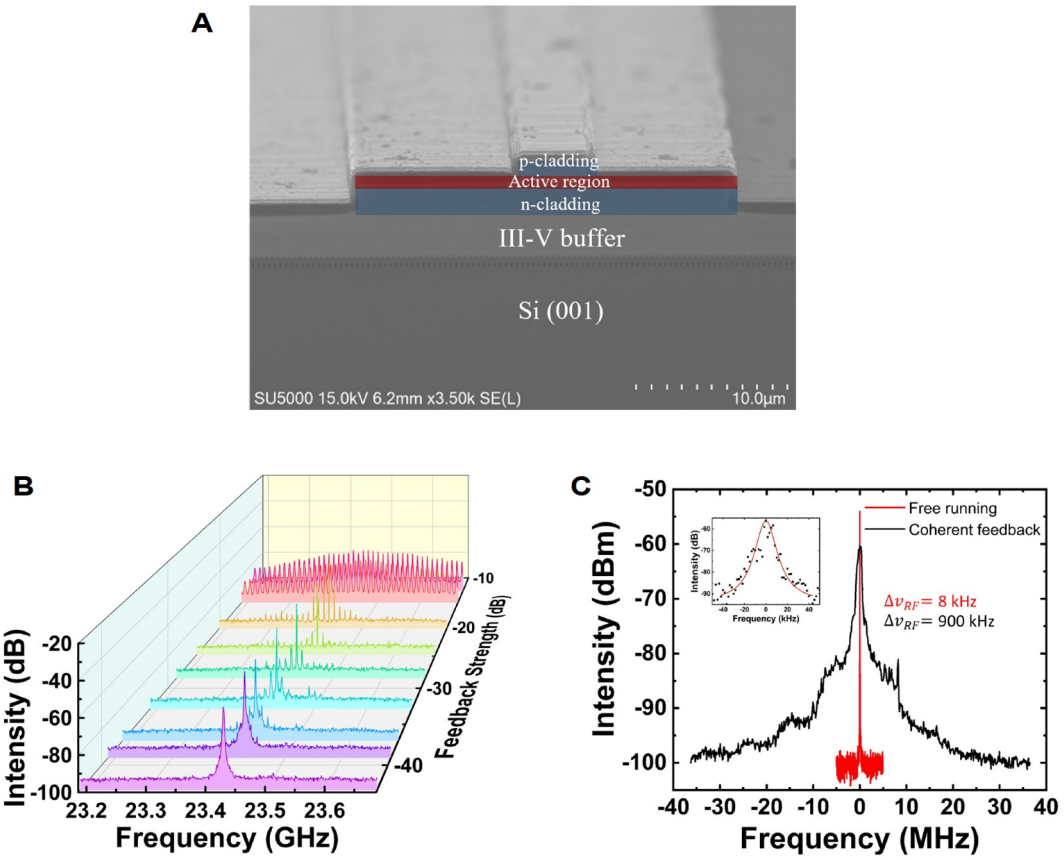

Figure 9 Si-based self-injection mode locked InAs/GaAs QD laser. (A) Color-enhanced SEM image of an initial Si-based ridge laser with the ridge width of 4 μm; (B) evolution of the RF spectra with different feedback strength; (C) the comparison of the RF spectra at 23.4 GHz of the MLL at mode-locked mode and free running mode.

The multi-wavelength injection locking of InAs/GaAs quantum dot FP lasers grown on silicon by optical self-injection via an external cavity was demonstrated recently as shown in Figure 10 [83]. By using chirped InAs QDs, an ultra-broad flat-top OFC spectrum was achieved from the FP laser on the Si substrate at the self-injection condition maintained by an external polarization-tunable fiber cavity as shown in Figure 10A. The number of locked laser modes can be fully adjusted from single peak to multiple peaks by tuning wavelength-dependent phase and mode spacing of back-injected light through Lyot filter, and the FSR of the OFCs is tunable from approximately 50 to 750 GHz. As shown in Figures 10B and 10C, at a low injection current of 75 mA, 10 self-injection locked peaks at comb spacing of 75 GHz (third-order) are achieved. While the injection current is increased up to 125 mA, relatively broad 3 dB bandwidth is presented in the

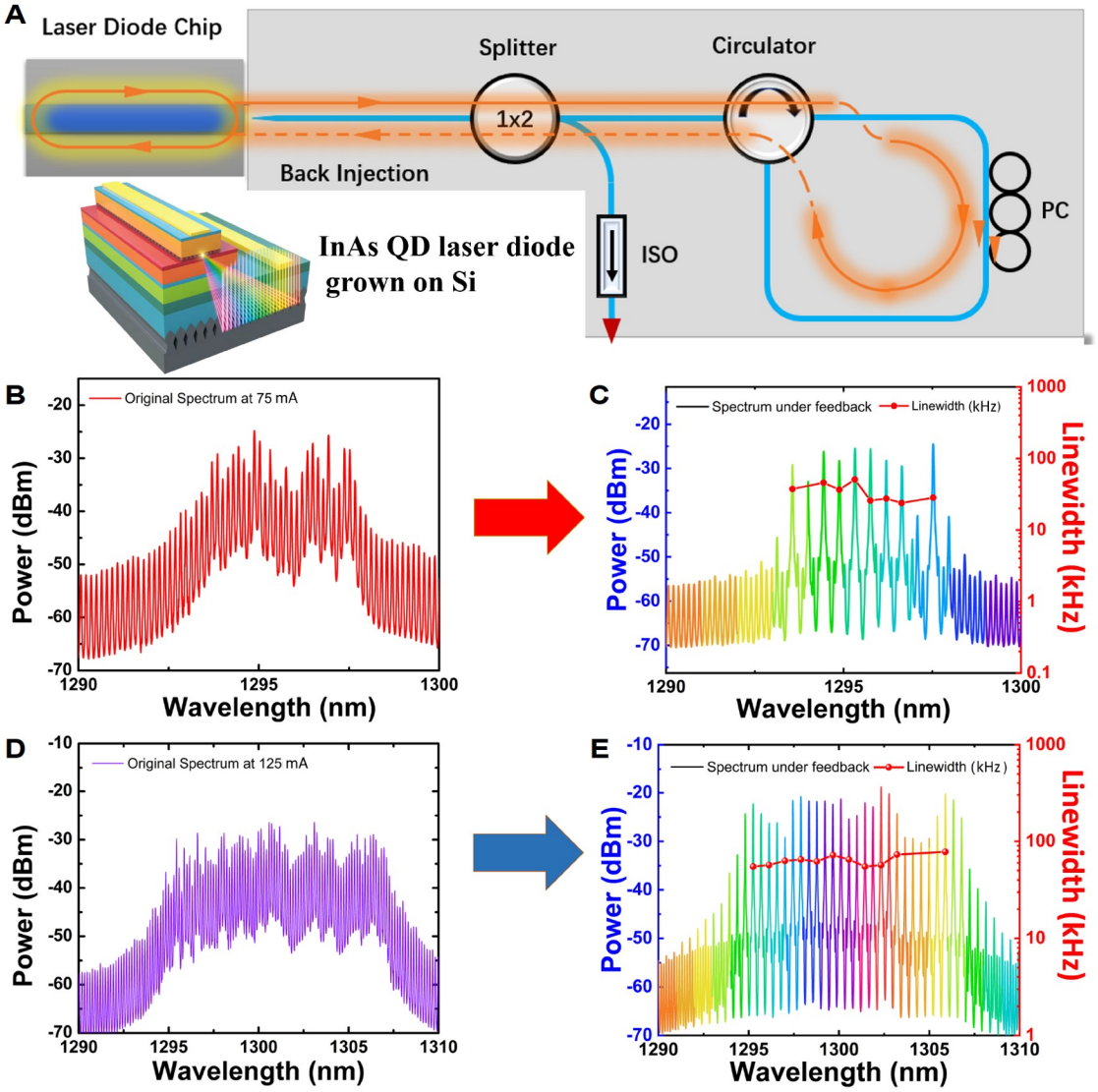

Figure 10 Si-based multi-wavelength self-injection InAs/GaAs QD MLLs with an external fiber cavity. (A) The schematics of chirped InAs QD laser on Si self-injection locked into multiple wavelengths via PM fiber based external cavity. Original optical spectrum (B) and the multi-wavelength injection locked comb spectrum (C) of the MLL operated at a low injection current of 75 mA. Original optical spectrum (D) and the multi-wavelength injection locked comb spectrum (E) of the MLL operated at a high injection current of 125 mA.

original optical spectrum; therefore, the number of injection locked comb lines is also increased to 30. The −10 dB bandwidth measured here is approximately 13 nm. Moreover, the optical linewidth of the combs is significantly narrowed by more than two orders of magnitude. It is the first report of multi-wavelength self-injection locked InAs QD FP laser on Si substrate with tunable FSR and large 10 dB bandwidth.

By implementing a standard QD FP laser diode epitaxially grown on Si with Lyot filter back-injection, narrow-linewidth flat-top comb laser with tunable FSR and large 10 dB bandwidth is demonstrated. Overall, Chen *et al*. [83] reported multi-wavelength self-injection locked InAs QD FP laser on Si substrate with tunable comb spacing depending on phase locking. These results pave the way towards tunable narrow-linewidth comb source for microwave photonics, photonic sensor system and quantum information applications.

CONCLUSIONS AND OUTLOOK

In this article, we have reviewed recent development of semiconductor MLL-based frequency comb generation. Compared with Kerr frequency combs, semiconductor MLLs exhibit essential advantages in comb power and power efficiency, but relative narrow gain bandwidth leads to their limited applications. Over octave bandwidth offers Kerr OFCs strong capability in precision measurements and sensing applications, but the sech^2 nature of soliton comb, which gives a large variation in single channel output power, remains a major drawback in WDM photonic interconnect applications. Therefore, at the current stage, MLL-based OFCs retain their advantages in foreseeable application fields such as DWDM telecommunications and optical interconnects. In order to extend the applications for semiconductor MLL generated comb sources, material systems with enlarged gain bandwidth need to be extensively developed in future research, such as chirped QD system or regrowth of multiple gain sections with extended wavelength. Overall, both semiconductor MLLs and Kerr OFCs exhibit their own unique physical properties that enable their targeted applications.

Data availability

The original data are available from corresponding authors upon reasonable request.

Funding

This work was supported by the National Natural Science Foundation of China (61975230 and 62008308) and the National Key Research and Development Program of China (2021YFB2800400). Ting Wang was supported by the Youth Innovation Promotion Association of the Chinese Academy of Sciences (2018011).

Conflict of interest

The authors declare that they have no conflict of interest.

References

1 Hargrove LE, Fork RL, Pollack MA. Locking of He–Ne laser modes induced by synchronous intracavity modulation. *Appl Phys Lett* 1964; **5**: 4–5.

2 Bloom BJ, Nicholson TL, Williams JR, *et al.* An optical lattice clock with accuracy and stability at the 10−18 level. *Nature* 2014; **506**: 71–75.

3 Fortier T, Baumann E. 20 years of developments in optical frequency comb technology and applications. *Commun Phys* 2019; **2**: 1–6.

4 Beloy K, Bodine MI. Frequency ratio measurements at 18-digit accuracy using an optical clock network. *Nature* 2021; **591**: 564–569.

5 Hall JL. Nobel lecture: Defining and measuring optical frequencies. *Rev Mod Phys* 2006; **78**: 1279–1295.

6 Thorpe MJ, Balslev-Clausen D, Kirchner MS, *et al.* Cavity-enhanced optical frequency comb spectroscopy: Application to human breath analysis. *Opt Express* 2008; **16**: 2387–2397.

7 Minoshima K, Matsumoto H. High-accuracy measurement of 240-m distance in an optical tunnel by use of a compact femtosecond laser. *Appl Opt* 2000; **39**: 5512–5517.

8 Hänsch TW. Nobel lecture: Passion for precision. *Rev Mod Phys* 2006; **78**: 1297–1309.

9 Hodgkinson J, Tatam RP. Optical gas sensing: A review. *Meas Sci Technol* 2012; **24**: 012004.

10 Nugent-Glandorf L, Giorgetta FR, Diddams SA. Open-air, broad-bandwidth trace gas sensing with a mid-infrared optical frequency comb. *Appl Phys B* 2015; **119**: 327–338.

11 Delfyett PJ, Gee S, Myoung-Taek Choi S, *et al.* Optical frequency combs from semiconductor lasers and applications in ultrawideband signal processing and communications. *J Lightwave Technol* 2006; **24**: 2701–2719.

12 Pfeifle J, Brasch V, Lauermann M, *et al.* Coherent terabit communications with microresonator Kerr frequency combs. *Nat Photon* 2014; **8**: 375–380.

13 Marin-Palomo P, Kemal JN, Karpov M, *et al.* Microresonator-based solitons for massively parallel coherent optical communications. *Nature* 2017; **546**: 274–279.

14 Lundberg L, Mazur M, Mirani A, *et al.* Phase-coherent lightwave communications with frequency combs. *Nat Commun* 2020; **11**: 1–7.

15 Diddams SA. The evolving optical frequency comb [invited]. *J Opt Soc Am B* 2010; **27**: B51.

16 Ito T, Nakamae H, Hazama Y, *et al.* Femtosecond pulse generation beyond photon lifetime limit in gain-switched semiconductor lasers. *Commun Phys* 2018; **1**: 42.

17 Weng W, Kaszubowska-Anandarajah A, He J, *et al.* Gain-switched semiconductor laser driven soliton microcombs. *Nat Commun* 2021; **12**: 1425.

18 Coluccelli N, Cassinerio M, Redding B, *et al.* The optical frequency comb fibre spectrometer. *Nat Commun* 2016; **7**: 1.

19 Pasquazi A, Peccianti M, Razzari L, *et al.* Micro-combs: A novel generation of optical sources. *Phys Rep* 2018; **729**: 1–81.

20 Gaeta AL, Lipson M, Kippenberg TJ. Photonic-chip-based frequency combs. *Nat Photon* 2019; **13**: 158–169.

21 Zhang M, Buscaino B, Wang C, *et al.* Broadband electro-optic frequency comb generation in a lithium niobate microring resonator. *Nature* 2019; **568**: 373–377.

22 Ren T, Zhang M, Wang C, *et al.* An integrated low-voltage broadband lithium niobate phase modulator. *IEEE Photon Technol Lett* 2019; **31**: 889–892.

23 Ho PT, Glasser LA, Ippen EP, *et al.* Picosecond pulse generation with a cw GaAlAs laser diode. *Appl Phys Lett* 1978; **33**: 241–242.

24 Huang X, Stintz A, Li H, *et al.* Passive mode-locking in 1.3 μm two-section InAs quantum dot lasers. *Appl Phys Lett* 2001; **78**: 2825–2827.

25 Koch BR, Fang AW, Cohen O, *et al.* Mode-locked silicon evanescent lasers. *Opt Express* 2007; **15**: 11225–11233.

26 Meng B, Singleton M, Shahmohammadi M, *et al.* Mid-infrared frequency comb from a ring quantum cascade laser. *Optica* 2020; **7**: 162–167.

27 Wang ZH, Wei WQ, Feng Q, *et al.* InAs/GaAs quantum dot single-section mode-locked lasers on Si (001) with optical self-injection feedback. *Opt Express* 2021; **29**: 674–683.

28 DeCusatis C M, Priest D G. Dense wavelength division multiplexing devices for metropolitan-area datacom and

telecom networks. In: *Proceedings of SPIE: Applications of Photonic Technology,* 2000. **4087**: 94–111.

29 Marin-Palomo P, Kemal JN, Kippenberg TJ, *et al.* Performance of chip-scale optical frequency comb generators in coherent WDM communications. *Opt Express* 2022; **28**: 12897–12910.

30 Li NX, Chen GY, Lim LW, *et al.* Fully integrated electrically driven optical frequency comb at communication wavelength. *Nanophotonics* 2022; **11**: 2989–3006.

31 Rickman A. The commercialization of silicon photonics. *Nat Photon* 2014; **8**: 579–582.

32 Thomson D, Zilkie A, Bowers JE, *et al.* Roadmap on silicon photonics. *J Opt* 2016; **18**: 073003.

33 Riemensberger J, Lukashchuk A, Karpov M, *et al.* Massively parallel coherent laser ranging using a soliton microcomb. *Nature* 2020; **581**: 164–170.

34 Diddams SA, Hollberg L, Mbele V. Molecular fingerprinting with the resolved modes of a femtosecond laser frequency comb. *Nature* 2007; **445**: 627–630.

35 Wang B, Morgan JS, Sun K, *et al.* Towards high-power, high-coherence, integrated photonic mmWave platform with microcavity solitons. *Light Sci Appl* 2021; **10**: 4.

36 Del'Haye P, Schliesser A, Arcizet O, *et al.* Optical frequency comb generation from a monolithic microresonator. *Nature* 2007; **450**: 1214–1217.

37 Hsieh IW, Chen X, Liu X, *et al.* Supercontinuum generation in silicon photonic wires. *Opt Express* 2007; **15**: 15242–15249.

38 Tucker RS, Koren U, Raybon G, *et al.* 40 GHz active mode-locking in a 1.5 μm monolithic extended-cavity laser. *Electron Lett* 1989; **25**: 621–622.

39 Griffith AG, Lau RKW, Cardenas J, *et al.* Silicon-chip mid-infrared frequency comb generation. *Nat Commun* 2015; **6**: 1–5.

40 Lee H, Chen T, Li J, *et al.* Chemically etched ultrahigh-Q wedge-resonator on a silicon chip. *Nat Photon* 2012; **6**: 369–373.

41 Levy JS, Gondarenko A, Foster MA, *et al.* CMOS-compatible multiple-wavelength oscillator for on-chip optical interconnects. *Nat Photon* 2010; **4**: 37–40.

42 Jung H, Xiong C, Fong KY, *et al.* Optical frequency comb generation from aluminum nitride microring resonator. *Opt Lett* 2013; **38**: 2810–2813.

43 Pu M, Ottaviano L, Semenova E, *et al.* Efficient frequency comb generation in AlGaAs-on-insulator. *Optica* 2016; **3**: 823–826.

44 He Y, Yang QF, Ling J, *et al.* Self-starting bi-chromatic $LiNbO_3$ soliton microcomb. *Optica* 2019; **6**: 1138–1144.

45 Guidry MA, Yang KY, Lukin DM, *et al.* Optical parametric oscillation in silicon carbide nanophotonics. *Optica* 2020; **7**: 1139–1142.

46 Asghari M, Krishnamoorthy AV. Energy-efficient communication. *Nat Photon* 2011; **5**: 268–270.

47 Lim AEJ, Liow TY, Song JF, et al. Path to silicon photonics commercialization: The foundry model discussion. In: *Silicon Photonics III. Berlin: Springer*, 2016. **122**: 191–215.

48 Haus HA. Mode-locking of lasers. *IEEE J Sel Top Quantum Electron* 2000; **6**: 1173–1185.

49 Bowers JE, Morton PA, Mar A, *et al.* Actively mode-locked semiconductor lasers. *IEEE J Quantum Electron* 1989; **25**: 1426–1439.

50 Chang L, Liu S, Bowers JE. Integrated optical frequency comb technologies. *Nat Photon* 2022; **16**: 95–108.

51 Menyuk CR, Wahlstrand JK, Willits J, *et al.* Pulse dynamics in mode-locked lasers: Relaxation oscillations and frequency pulling. *Opt Express* 2007; **15**: 6677–6689.

52 Derickson DJ, Helkey RJ, Mar A, *et al.* Short pulse generation using multisegment mode-locked semiconductor lasers. *IEEE J Quantum Electron* 1992; **28**: 2186–2202.

53 Chen YK, Wu MC, Tanbun-Ek T, *et al.* Subpicosecond monolithic colliding-pulse mode-locked multiple quantum well lasers. *Appl Phys Lett* 1991; **58**: 1253–1255.

54 Liu S, Jung D, Norman JC, *et al.* 490 fs pulse generation from passively mode-locked single section quantum dot laser

directly grown on on-axis GaP/Si. *Electron lett* 2018; **54**: 432–433.

55 Khurgin JB, Dikmelik Y, Hugi A, *et al.* Coherent frequency combs produced by self-frequency modulation in quantum cascade lasers. *Appl Phys Lett* 2014; **104**: 081118.

56 Liang W, Ilchenko VS, Eliyahu D, *et al.* Ultralow noise miniature external cavity semiconductor laser. *Nat Commun* 2015; **6**: 7371.

57 Watanabe H, Miyajima T, Kuramoto M, *et al.* 10-W peak-power picosecond optical pulse generation from a triple section blue-violet self-pulsating laser diode. *Appl Phys Express* 2010; **3**: 052701.

58 Martins-Filho JF, Avrutin EA, Ironside CN, *et al.* Monolithic multiple colliding pulse mode-locked quantum-well lasers, experiment and theory. *IEEE J Sel Top Quantum Electron* 1995; **1**: 539–551.

59 Marsh JH, Hou L. Mode-locked laser diodes and their monolithic integration. *IEEE J Sel Top Quantum Electron* 2017; **23**: 1–11.

60 Norman JC, Jung D, Zhang Z, *et al.* A review of high-performance quantum dot lasers on silicon. *IEEE J Quantum Electron* 2019; **55**: 1–11.

61 Rafailov EU, Cataluna MA, Sibbett W. Mode-locked quantum-dot lasers. *Nat Photon* 2007; **1**: 395–401.

62 Bimberg D, Pohl UW. Quantum dots: Promises and accomplishments. *Mater Today* 2011; **14**: 388–397.

63 Kageyama T, Nishi K, Yamaguchi M, *et al*. Extremely high temperature (220 °C) continuous-wave operation of 1300-nm-range quantum-dot lasers. In: *Proceedings of the European Conference on Lasers and Electro-Optics*, 2011. PDA_1.

64 Liu AY, Srinivasan S, Norman J, *et al.* Quantum dot lasers for silicon photonics [Invited]. *Photon Res* 2015; **3**: B1.

65 Liu AY, Komljenovic T, Davenport ML, *et al.* Reflection sensitivity of 13 μm quantum dot lasers epitaxially grown on silicon. *Opt Express* 2017; **25**: 9535–9543.

66 Schmeckebier H, Bimberg D. Quantum-dot semiconductor optical amplifiers for energy-efficient optical communication. In: *Green Photon Electron*. Cham: Springer, 2017. 37–74.

67 Arsenijević D, Bimberg D. Quantum-dot mode-locked lasers: Sources for tunable optical and electrical pulse combs. In: *Green Photon Electron*. Cham: Springer, 2017. 75–106.

68 Duan JN, Wang XG, Zhou YG, *et al*. Relative intensity noise properties of quantum dot lasers. *In: Proceedings of SPIE Semiconductor Lasers and Applications VIII*, 2018. 10812S.

69 Liu S, Wu X, Jung D, *et al.* High-channel-count 20 GHz passively mode-locked quantum dot laser directly grown on Si with 41 Tbit/s transmission capacity. *Optica* 2019; **6**: 128–134.

70 Hugi A, Villares G, Blaser S, *et al.* Mid-infrared frequency comb based on a quantum cascade laser. *Nature* 2012; **492**: 229–233.

71 Wang CY, Kuznetsova L, Gkortsas VM, *et al.* Mode-locked pulses from mid-infrared quantum cascade lasers. *Opt Express* 2009; **17**: 12929–12943.

72 Novus Light Technologies Today, News and analysis from the world of light. *https://www.novuslight.com/advanced-indium-phosphide-pdk-for-photonic-integrated-circuit-designN6729.html* (20 March 2017, date last accessed).

73 Wang ZC, Van Gasse K, Moskalenko V, *et al.* A III-V-on-Si ultra-dense comb laser. *Light Sci Appl* 2017; **6**: e16260.

74 Cuyvers S, Haq B, Op de Beeck C, *et al.* Low noise heterogeneous III-V-on-silicon-nitride mode-locked comb laser. *Laser Photonics Rev* 2021; **15**: 2000485.

75 Kurczveil G, Zhang C, Descos A, *et al*. On-chip hybrid silicon quantum dot comb laser with 14 error-free channels. In: *Proceedings of IEEE International Semiconductor Laser Conference (ISLC)*, 2018. 1–2.

76 Liu S, Wu X, Norman J, *et al*. 100 GHz colliding pulse mode locked quantum dot lasers directly grown on Si for WDM application. In: *Proceedings of Conference on Lasers and Electro-Optics (CLEO)*, 2019. ATu3P. 5.

77 Pan SJ, Huang JO, Zhou ZC, *et al.* Quantum dot mode-locked frequency comb with ultra-stable 25.5 GHz spacing between 20°C and 120°C. *Photon Res* 2020; **8**: 1937–1942.

78 Pan S, Zhang H, Liu Z, *et al.* Multi-wavelength 128 Gbit s^{-1} λ^{-1} PAM4 optical transmission enabled by a 100 GHz quantum dot mode-locked optical frequency comb. *J Phys D-Appl Phys* 2022; **55**: 144001.

79 Huang JZ, Ji ZT, Chen JJ, *et al.* Ultra-broadband flat-top quantum dot comb lasers. *Photon Res* 2022; **10**: 1308–1316.

80 Jin W, Yang QF, Chang L, *et al.* Hertz-linewidth semiconductor lasers using CMOS-ready ultra-high-Q microresonators. *Nat Photonics* 2021; **15**: 346–353.

81 Pavlov NG, Koptyaev S, Lihachev GV, *et al.* Narrow-linewidth lasing and soliton Kerr microcombs with ordinary laser diodes. *Nat Photon* 2018; **12**: 694–698.

82 Raja AS, Voloshin AS, Guo H, *et al.* Electrically pumped photonic integrated soliton microcomb. *Nat Commun* 2019; **10**: 680.

83 Chen JJ, Wei WQ, Qin JL, *et al.* Multi-wavelength injection locked semiconductor comb laser. *Photon Res* 2022; **10**: 1840.

84 Pan S, Zhang H, Wu D, *et al*. O-band 100 GHz quantum dot mode-locked optical frequency comb with 128 Gbit/s/ λ PAM-4 optical transmission ability. In: *Proceedings of Asia Communications and Photonics Conference*, 2021. T4D.7.

85 Arakawa Y, Sakaki H. Multidimensional quantum well laser and temperature dependence of its threshold current. *Appl Phys Lett* 1982; **40**: 939–941.

86 Cataluna MA, Rafailov EU, McRobbie AD, *et al.* Stable mode-locked operation up to 80 /spl deg/C from an InGaAs quantum-dot laser. *IEEE Photon Technol Lett* 2006; **18**: 1500–1502.

87 Liang D, Bowers JE. Recent progress in heterogeneous III-V-on-silicon photonic integration. *Light: Adv Manuf* 2021; **2**: 59–83.

88 Ramírez JM, Fanneau de la Horie P, Provost JG, *et al.* Low-threshold, high-power on-chip tunable III-V/Si lasers with integrated semiconductor optical amplifiers. *Appl Sci* 2021; **11**: 11096.

89 Kurczveil G, Liang D, Fiorentino M, *et al.* Robust hybrid quantum dot laser for integrated silicon photonics. *Opt Express* 2016; **24**: 16167–16174.

90 Kurczveil G, Seyedi MA, Liang D, *et al.* Error-free operation in a hybrid-silicon quantum dot comb laser. *IEEE Photon Technol Lett* 2018; **30**: 71–74.

91 Dong B, Huang H, Duan J, *et al.* Frequency comb dynamics of a 13 μm hybrid-silicon quantum dot semiconductor laser with optical injection. *Opt Lett* 2019; **44**: 5755–5758.

92 Li Q, Lau KM. Epitaxial growth of highly mismatched III-V materials on (001) silicon for electronics and optoelectronics. *Prog Cryst Growth Charact Mater* 2017; **63**: 105–120.

93 Wei W, Feng Q, Wang Z, *et al.* Perspective: Optically-pumped III–V quantum dot microcavity lasers via CMOS compatible patterned Si (001) substrates. *J Semicond* 2019; **40**: 101303.

94 Wang T, Liu H, Lee A, *et al.* 13-μm InAs/GaAs quantum-dot lasers monolithically grown on Si substrates. *Opt Express* 2011; **19**: 11381–11386.

95 Liu H, Wang T, Jiang Q, *et al.* Long-wavelength InAs/GaAs quantum-dot laser diode monolithically grown on Ge substrate. *Nat Photon* 2011; **5**: 416–419.

96 Liu AY, Peters J, Huang X, *et al.* Electrically pumped continuous-wave 13 μm quantum-dot lasers epitaxially grown on on-axis (001) GaP/Si. *Opt Lett* 2017; **42**: 338–341.

97 Kwoen J, Jang B, Lee J, *et al.* All MBE grown InAs/GaAs quantum dot lasers on on-axis Si (001). *Opt Express* 2018; **26**: 11568–11576.

98 Norman J, Kennedy MJ, Selvidge J, *et al.* Electrically pumped continuous wave quantum dot lasers epitaxially grown on patterned, on-axis (001) Si. *Opt Express* 2017; **25**: 3927–3934.

99 Chen S, Li W, Wu J, *et al.* Electrically pumped continuous-wave III–V quantum dot lasers on silicon. *Nat Photon* 2016; **10**: 307–311.

100 Li Q, Ng KW, Lau KM. Growing antiphase-domain-free GaAs thin films out of highly ordered planar nanowire arrays on exact (001) silicon. *Appl Phys Lett* 2015; **106**: 072105.

101 Alcotte R, Martin M, Moeyaert J, *et al.* Epitaxial growth of antiphase boundary free GaAs layer on 300 mm Si(001) substrate by metalorganic chemical vapour deposition with high mobility. *APL Mater* 2016; **4**: 046101.

102 Wei WQ, Wang JH, Zhang B, *et al.* InAs QDs on (111)-faceted Si (001) hollow substrates with strong emission at

1300 nm and 1550 nm. *Appl Phys Lett* 2018; **113**: 053107.

103 Zhang B, Wei WQ, Wang JH, *et al.* 1310 nm InAs quantum-dot microdisk lasers on SOI by hybrid epitaxy. *Opt Express* 2019; **27**: 19348–19358.

104 Wei WQ, Zhang JY, Wang JH, *et al.* Phosphorus-free 15 μm InAs quantum-dot microdisk lasers on metamorphic InGaAs/SOI platform. *Opt Lett* 2020; **45**: 2042.

105 Wei WQ, Feng Q, Guo JJ, *et al.* InAs/GaAs quantum dot narrow ridge lasers epitaxially grown on SOI substrates for silicon photonic integration. *Opt Express* 2020; **28**: 26555.